

Self-Assembled Monolayers of Metal-Assembling Dendron Thiolate Formed from Dendrimers with a Disulfide Core

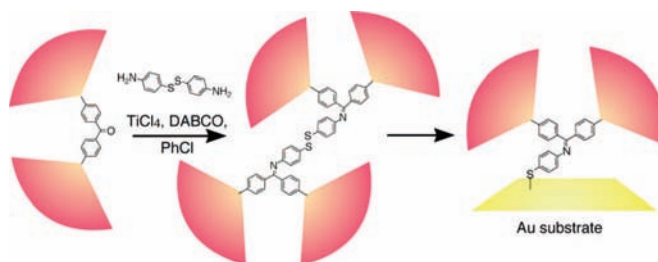
Norifusa Satoh and Kimihisa Yamamoto*

Department of Chemistry, Faculty of Science & Technology, Keio University,
Yokohama 223-8522, Japan

yamamoto@chem.keio.ac.jp

Received January 21, 2009

ABSTRACT



Novel phenylazomethine dendrimers with a disulfide core (SS-DPA G1–4) were synthesized in nearly quantitative yields. Although the disulfide core is shielded by the rigid dendron shell, direct formation of the self-assembled monolayers of metal-assembling dendron thiolate was observed by XPS and electrochemical reduction of the self-assembled monolayer substrates. The dendrimers showed a similar metal-assembling manner with other derivatives. The metal assembly to the self-assembled monolayers of metal-assembling dendron thiolate was also confirmed.

Self-assembled monolayers (SAMs) have attracted much attention for designing functional surfaces in the fields of chemical and biochemical sensing and nanopatterning for molecular electronics.¹ In particular, the combination of SAMs with metal assembly on the surfaces has been applied to electron transporters and sensors.² Additionally, dendrimers have been strictly used as a functional surfactant because of their regulated structure,^{3,4} which allow the construction of finely controlled surfaces.

We now report the synthesis of phenylazomethine dendrimers with a disulfide core (SS-DPAs) and direct formation

of the dendron thiolate SAMs from the dendrimers. The π -conjugated structure would improve the thermostability⁵ and electron transport^{6,7} in the SAM structure. Additionally, we found that the SS-DPAs showed a stepwise metal

(1) (a) Ulman, A. *Chem. Rev.* **1996**, *96*, 1533. (b) Joachim, C.; Gimzewski, J. K.; Aviram, A. *Nature* **2000**, *408*, 541. (c) Love, J. C.; Estroff, L. A.; Kriebel, J. K.; Nuzzo, R. J.; Whitesides, G. M. *Chem. Rev.* **2005**, *105*, 1103.

(2) (a) Maskus, M.; Abruna, H. D. *Langmuir* **1996**, *12*, 4455. (b) Abe, M.; Michi, T.; Sato, A.; Kondo, T.; Zhou, W.; Ye, S.; Uosaki, K.; Sasaki, Y. *Angew. Chem., Int. Ed.* **2003**, *42*, 2912. (c) Kanaizuka, K.; Murata, M.; Nishimori, Y.; Mori, I.; Nishio, K.; Masuda, H.; Nishihara, H. *Chem. Lett.* **2005**, *34*, 534.

(3) (a) Gorman, C. B.; Miller, R. L.; Chen, K.-Y.; Bishop, A. R.; Haasch, R. T.; Nuzzo, R. G. V. *Langmuir* **1998**, *14*, 3312. (b) Zhang, L.; Huo, F.; Wang, Z.; Wu, L.; Zhang, X.; Höppener, S.; Chi, L.; Fuchs, H.; Zhao, J.; Niu, L.; Dong, S. *Langmuir* **2000**, *16*, 3813. (c) Friggeri, A.; Schönherr, H.; van Manen, H.-J.; Huisman, B.-H.; Vancso, G. J.; Huskens, J.; van Veggel, F. C. J. M.; Reinhoudt, D. N. *Langmuir* **2000**, *16*, 7757. (d) Zhang, L.; Zou, B.; Dong, B.; Huo, F.; Zhang, X.; Chi, L.; Jiang, L. *Chem. Commun.* **2001**, 1906. (e) Mark, S. S.; Sandhyarani, N.; Zhu, C.; Campagnolo, C.; Batt, C. A. *Langmuir* **2004**, *20*, 6808.

(4) (a) Taranekekar, P.; Baba, A.; Park, J. Y.; Fulghum, T. M.; Advincula, R. *Adv. Funct. Mater.* **2006**, *16*, 2000. (b) Nishimori, Y.; Kanaizuka, K.; Murata, M.; Nishihara, H. *Chem. Asian J.* **2007**, *2*, 367.

(5) Ishida, T.; Fukushima, H.; Mizutani, W.; Miyashita, S.; Ogiso, H.; Ozaki, K.; Tokumoto, H. *Langmuir* **2002**, *18*, 83.

(6) (a) Choi, S. H.; Kim, B.-S.; Frisbie, C. D. *Science* **2008**, *320*, 1482. (b) Yamamoto, K.; Higuchi, M.; Uchida, K.; Kojima, Y. *Macromolecules* **2002**, *35*, 5782.

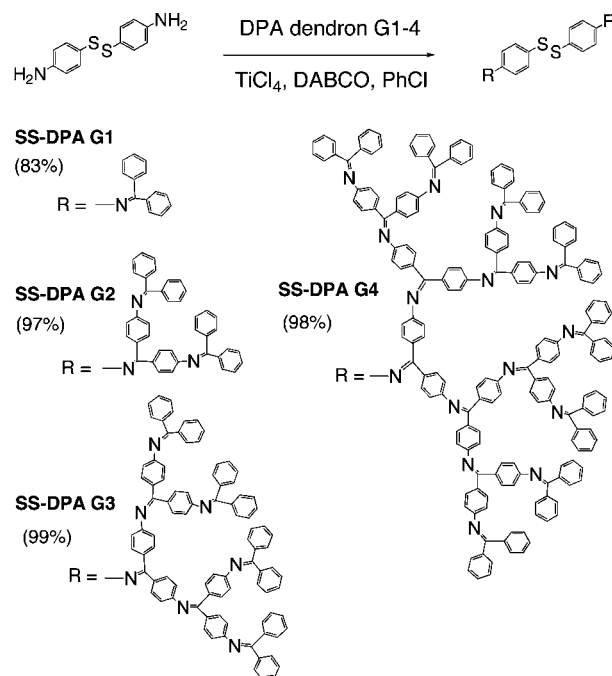
assembly.⁸ These properties should allow the construction of novel functional surfaces.

The phenylazomethine dendrimers (DPAs) with a phenyl-based core were synthesized up to the fifth generation by a convergent method via the reaction of aromatic ketones with aromatic amines.⁹ The DPA derivatives are synthesized by the reaction between the DPA dendrons containing an aromatic ketone and the core compound having some aromatic amines.^{7a,d,10} Thus, we dehydrated di-*p*-diaminophenyldisulfide with the DPA dendrons, G1–4, in the presence of titanium(IV) tetrachloride and 1,4-diazabicyclo[2.2.2]octane (DABCO) to synthesize the disulfide core dendrimers (SS-DPA G1–4, Scheme 1).

The MALDI-TOF mass spectra of the dendrimers showed two peaks of the calculated mass and half the mass (Table 1 and Figure S3a). This fact strongly indicates that the dendrimers have a disulfide unit at the core.¹¹ In contrast, size exclusion chromatography (SEC) of the dendrimers showed a single peak ($M_w/M_n = 1.02$, Table 1 and Figure S3b, Supporting Information). Additionally, the absolute molecular weight, analyzed by a triple detector (a differential viscometer, laser light scattering, and an RI detector: Viscotek Corp.),¹² agrees with the calculated mass (Table 1). Thus, we determined that the obtained dendrimers have a single molecular weight and a disulfide unit.

The yield of all the generations of the dendrimers was almost quantitative;¹³ this result means that the contact for dehydration between the aromatic amines of the core and the aromatic ketone of the dendron would not be three-dimensionally hindered by the growth of the dendron size because of the free rotation of the disulfide bond. The yield

Scheme 1. Synthesis of SS-DPAs



of the previous dendrimer derivatives having a rigid core, such as a phenyl and tris(thienylphenyl)amine core (DPAs and TPA-DPAs), decreases with the generation number.^{7a,d,10}

The molecular structure of the dendritic molecules closely relates to the intrinsic viscosity ($[\eta]$).¹⁴ Figure S4a (Supporting Information) shows Mark–Houwink plots of the SS-DPAs (Mark–Houwink–Sakurada equation: $[\eta] = K M^a$). The slopes of these plots (Mark–Houwink exponent; a) gradually change but do not reach zero. In contrast, we have confirmed that the Mark–Houwink exponent of the higher generations of DPAs and TPA-DPAs clearly changes to nearly zero, which means that these dendrimers have a rigid spherical structure like a globular protein.^{7a,d} Thus, we can conclude that only one flexible unit at the core dramatically changes the structural conformation of the rigid dendrimers.

The changes in the structural properties were also observed in the hydrodynamic radii (R_h) of these dendrimers, obtained from the triple detector analysis (Table 1 and Figure S4b, Supporting Information). The radius linearly increased with the generation number because of the rigid branched units. The generational increase in the radius is consistent with the modeling size of the branched units. Thus, the rigid molecular chain would radially grow and shield the core (the modeling structure of SS-DPA G4 is shown in Figure S5, Supporting Information).^{15,16} However, the difference in the radii

(7) Metal assembly into the dendrimers also improves the hole-transfer: (a) Satoh, N.; Cho, J.-S.; Higuchi, M.; Yamamoto, K. *J. Am. Chem. Soc.* **2003**, *125*, 8104. (b) Kimoto, K.; Masachika, K.; Cho, J.-S.; Higuchi, M.; Yamamoto, K. *Chem. Mater.* **2004**, *16*, 5706. (c) Kimoto, A.; Cho, J.-S.; Higuchi, M.; Yamamoto, K. *Macromolecules* **2004**, *37*, 5531. (d) Satoh, N.; Nakashima, T.; Yamamoto, K. *J. Am. Chem. Soc.* **2005**, *127*, 13030. (e) Cho, J.-S.; Takanashi, K.; Higuchi, M.; Yamamoto, K. *Synth. Met.* **2005**, *1*, 79. (f) Nakashima, T.; Satoh, N.; Albrecht, K.; Yamamoto, K. *Chem. Mater.* **2008**, *20*, 2538. (g) Kimoto, A.; Cho, J.-S.; Ito, K.; Aoki, D.; Miyake, T.; Yamamoto, K. *Macromol. Rapid Commun.* **2005**, *26*, 597.

(8) (a) Yamamoto, K.; Higuchi, M.; Shiki, S.; Tsuruta, M.; Chiba, H. *Nature* **2002**, *415*, 509. (b) Nakajima, R.; Tsuruta, T.; Higuchi, M.; Yamamoto, K. *J. Am. Chem. Soc.* **2004**, *126*, 1630. (c) Satoh, N.; Watanabe, T.; Iketaki, Y.; Omatsu, T.; Fujii, M.; Yamamoto, K. *Polym. Adv. Technol.* **2004**, *15*, 159. (d) Takanashi, K.; Fujii, A.; Nakajima, R.; Chiba, H.; Higuchi, M.; Einaga, Y.; Yamamoto, K. *Bull. Chem. Soc. Jpn.* **2007**, *80*, 1563. (e) Yamamoto, K.; Kawana, Y.; Tsuji, M.; Hayashi, M.; Imaoka, T. *J. Am. Chem. Soc.* **2007**, *129*, 9256. (f) Satoh, N.; Nakashima, T.; Kamikura, K.; Yamamoto, K. *Nature Nanotech.* **2008**, *3*, 106.

(9) (a) Higuchi, M.; Shiki, S.; Yamamoto, K. *Org. Lett.* **2000**, *2*, 3079. (b) Takanashi, K.; Chiba, H.; Higuchi, M.; Yamamoto, K. *Org. Lett.* **2004**, *6*, 1709. (c) Higuchi, M.; Kanazawa, H.; Tsuruta, M.; Yamamoto, K. *Macromolecules* **2001**, *34*, 8847.

(10) (a) Higuchi, M.; Shiki, S.; Ariga, K.; Yamamoto, K. *J. Am. Chem. Soc.* **2001**, *123*, 4414. (b) Imaoka, T.; Horiguchi, H.; Yamamoto, K. *J. Am. Chem. Soc.* **2003**, *125*, 340. (c) Enoki, O.; Imaoka, T.; Yamamoto, K. *Org. Lett.* **2003**, *5*, 2547. (d) Enoki, O.; Katoh, H.; Yamamoto, K. *Org. Lett.* **2006**, *8*, 569.

(11) Gorman, J. J.; Wallis, T. P.; Pitt, J. J. *Mass Spectrom. Rev.* **2002**, *21*, 183.

(12) (a) Yau, W. W.; Rementer, S. W. *J. Liq. Chromatogr.* **1990**, *13*, 627. (b) Jackson, C.; Yau, W. W. *J. Chromatogr.* **1993**, *645*, 209. (c) Jackson, C.; Yau, W. W. *Adv. Chem. Ser.* **1995**, *247*, 69.

(13) The yield of SS-DPA G1 is the lowest (83%) because of the solubility to methanol in the reprecipitation process.

(14) (a) Tomalia, D. A.; Naylor, A. M.; Goddard, W. A., III. *Angew. Chem., Int. Ed. Engl.* **1990**, *29*, 138. (b) Tomalia, D. A. *Prog. Polym. Sci.* **2005**, *30*, 294.

(15) Gorman, C. B.; Smith, J. C.; Hager, M. W.; Parkhurst, B. L.; Sierzputowska-Gracz, H.; Haney, C. A. *J. Am. Chem. Soc.* **1999**, *121*, 9958.

(16) Saeki, A.; Seki, S.; Satoh, N.; Yamamoto, K.; Tagawa, S. *J. Phys. Chem. B* **2008**, *112*, 15540. (b) Yan, X.-Z.; Goodson, T.; Imaoka, T.; Yamamoto, K. *J. Phys. Chem. B* **2005**, *109*, 9321.

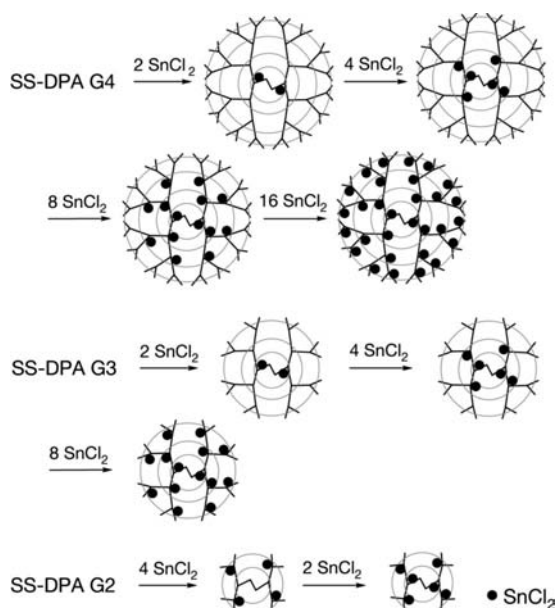


Figure 1. Schematic representation of stepwise complexation into the SS-DPAs.

between the DPAs and SS-DPAs is quite small (0.48 Å as average), compared with the difference in the chemical structure of these cores.^{7a,d} This also suggests the flexibility of the disulfide core.

The rigid branched units provide a high thermostability to the DPA derivatives (Table 1 and Figure S6, Supporting Information).¹⁷ The 10 weight % decreasing temperatures ($T_{d-10\%}$) and the glass transition temperatures (T_g) of the SS-DPAs improved with the increase in the generation number, reaching 505 and 158 °C, respectively. Thus, we noticed that the SS-DPAs have a high thermostability as SAM molecules, comparable to engineering plastics. However, the SS-DPAs have a lower thermostability by 10–20 °C than the DPAs and the other derivatives having a rigid and dense structure, such as porphine, with a similar molecular weight.^{17a} A similar tendency was also observed in the TPA-DPAs because of the central space around the core.^{17b} Thus, the thermostability of the SS-DPAs would decrease due to the mobility at the disulfide core.

The metal-assembling property of the SS-DPAs, based on the complexation between the imine ligands and SnCl_2 in this case, was confirmed by spectroscopic measurements (Figure S7–9, Supporting Information). The absorption band around 400 nm, attributed to the complexation, increases with a decrease in the absorption bands around 320 nm that are attributed to the phenylazomethine unit. During the addition of SnCl_2 , we found a stepwise complexation behavior of the SS-DPAs similar to that of the DPA derivatives having electron-withdrawing cores, such as the tetrafluorophenyl and

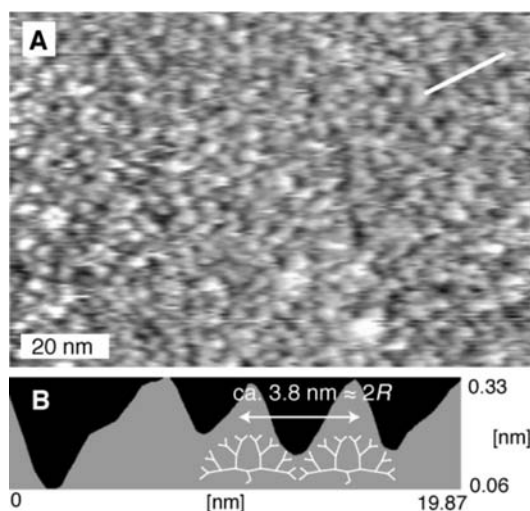


Figure 2. (A) STM image and (B) the cross section of SAM fabricated from SS-DPA G4; $I = 50$ pA, $V_{\text{sample}} = 1.0$ V.

2,5-dichlorophenyl cores.¹⁸ However, the “reversed” pattern of complexation was observed in only SS-DPA G2 because of the very weak electron withdrawing nature of the disulfide core. We confirmed that the complexation to the disulfide core is never detected by the ^1H NMR spectral changes (Figure S10, Supporting Information).

For SS-DPA G3 and SS-DPA G4, the radial stepwise complexation of SnCl_2 was observed until a stoichiometric amount (per imine site) of SnCl_2 had been added. Four and three distinct transitions could be identified at the isosbestic points—363 nm, 0–2 equiv; 361 nm, 3–6 equiv; 358 nm, 7–14 equiv; 353 nm, 15–30 equiv for SS-DPA G4 (Figure S7, Supporting Information); 363 nm, 0–2 equiv; 361 nm, 3–6 equiv; 358 nm, 7–14 equiv for SS-DPA G3 (Figure S8, Supporting Information), respectively—indicating that the complexation proceeds in a stepwise manner rather than randomly. The existence of an isosbestic point reveals the quantitative transformation of the compound, so the observation of four and three distinct isosbestic points suggests the successive formation of four and three different complexes upon the addition of SnCl_2 , respectively. The number of added equivalents of SnCl_2 at each transition is consistent with the number of imine sites present in the different layers from the inner position of the SS-DPA G3 and SS-DPA G4, respectively (Figure 1).

For SS-DPA G2, the two isosbestic points were observed during the titration—363 nm, 0–4 equiv.; 361 nm, 5–6 equiv. (Figure S9, Supporting Information)—indicating that the complexation for the second layer was completed first, and then the first layer was filled (Figure 1). This stepwise complexation reflects the basicity of the imines in each layer of the system, which is confirmed in the ^{13}C NMR spectra (Figure S11, Supporting Information); the high magnetic field shift of the imine carbon peaks attributed to the electron-

(17) (a) Tanaka, R.; Imaoka, T.; Yamamoto, K. *J. Photopolym. Sci. Tech.* **2004**, *17*, 323. (b) Satoh, N.; Cho, J.-S.; Higuchi, M.; Yamamoto, K. *J. Photopolym. Sci. Tech.* **2005**, *18*, 55.

(18) Higuchi, M.; Tsuruta, T.; Chiba, H.; Shiki, S.; Yamamoto, K. *J. Am. Chem. Soc.* **2003**, *125*, 9988.

Table 1. Physicochemical Characteristics of SS-DPAs

SS-DPA	yield (%)	$M_{\text{cal.}}$	TOF-MS ^a		Tri-SEC ^b				TG-DSC ^c	
			M/z		M_n^d	M_w/M_n^e	R_h (nm)	log {[η] (dL/g)}	$T_{\text{d-10\%}}$ (°C)	T_g (°C)
G1	83	576.77	576.4	287.7	580	1.02	0.64	−1.493	—	19
G2	97	1293.64	1292.4	646.1	1290	1.02	0.93	−1.374	419	77
G3	99	2727.38	2727.1	1363.1	2760	1.03	1.30	−1.305	495	128
G4	98	5594.86	5595.5	2795.8	5600	1.02	1.66	−1.260	505	158

^a MALDI-TOF mass spectroscopy. ^b SEC analyzed with a triple detector. ^c Thermogravimetry/Differential scanning calorimetry. ^d Number average molecular weight. ^e Molecular weight distribution.

donated imine, showing the faster complexation with SnCl_2 .¹⁸ The carbon peak of the first layer imines of the SS-DPAs showed a downfield shift when compared with that of the DPAs. The downfield shift, however, is smaller than that of the DPA derivatives having a tetrafluorophenyl or 2,5-dichlorophenyl core. Thus, the carbon peak of the first layer imines of SS-DPA G2 appeared at a lower field than that of the second layer ones, although the carbon peak of SS-DPA G3 shifted to the highest field for the imine peaks because of the electron donation by the outer layer's imines. These phenomena agree with the complexation manner in the SS-DPAs.

Absorption of the dendrimer on a Au substrate was observed by AFM (Figure S12, Supporting Information). The disulfide core as a binding site to form the SAM structure is shielded by the rigid dendron. Thus, the SAM formation was delayed by the rigid shell as the generation number increases. The amounts of the SAM molecules covering on Au substrates after the 1 h, 2 h, and 3 h soaks in the solution of SS-DPA G1, G2, and G3 were estimated from the AFM images; the initial formation rate constants were calculated to be 0.30, 0.21, and 0.06 h^{-1} at room temperature, respectively. The full coverage under SS-DPA G4 conditions was observed after a 2-days soak (STM image shown in Figure 2), indicating that the rate constant was estimated to be ca. 0.02 h^{-1} at room temperature. The observed molecular size was estimated to be ca. 3.8 nm, comparable to the hydrodynamic diameter of the SS-DPA G4. The highly ordered structure would be obtained by annealing or a change in the soak conditions.

Formation of the Au–S bond was confirmed by the XPS spectra and the electrochemical reduction of the fully covered SAM substrate. The binding energy of $\text{S}(2p_{3/2})$ showed a difference between the dendrimer cast film (163 eV; Figure S13a, Supporting Information) and the SAM film (162 eV; Figure S13b, Supporting Information). This shift indicates the occurrence of the following reaction: $1/2 \text{R-S-S-R} + \text{Au}_{(\text{surface})} \rightarrow \text{R-S}^-\cdot\text{Au}^+_{(\text{surface})}$. Additionally, the reduction current of the $\text{Au}^+_{(\text{surface})}$ was observed at 0.6 V in the cyclic voltammogram of the SAM substrate (Figure S14a, Supporting Information). After three cycles, the amount of the binding SAM molecules decreased to 5% because of the release of the SAM molecules (Figure S14b, Supporting Information). These results indicate that the dendron thiolate

SAM directly forms from the dendrimers shielding the disulfide core at the center, although the formation is disturbed by the rigid shell.

The metal assembly into the SAM structure was observed in the differential UV–vis spectra after the addition of SnCl_2 in acetonitrile (Figure S15, Supporting Information). The increase in the absorption band (350–550 nm) is characteristic of the complexation.¹⁹ The spectral changes indicate that the dendron thiolates on Au substrate would maintain the metal-assembling properties, although the assembling manner is unclear.

In summary, we have synthesized up to the fourth generation of the SS-DPAs in near quantitative yields. The only one flexible unit at the core dramatically affects the structural conformation of the π -conjugated dendrimers, resulting in a high yield. The hydrodynamic radius linearly increases with the generation number because of the rigid dendron shell. The π -conjugated structure contributes to the thermostabilities. The UV–vis spectra changes by the addition of SnCl_2 revealed that the metal assembly into the dendrimers is similar to the other DPA derivatives. It is supported by the chemical shift in the imine carbon peaks of the ^{13}C NMR spectra. Similar spectral changes were also observed for the metal assembly into the dendron thiolate SAMs.

Acknowledgment. This work was partially supported by CREST from the Japan Science and Technology Agency, Grants-in-Aid for Scientific Research (No. 19205020) and the 21st Center of Excellence (COE) Program (Keio-LCC) from the Ministry of Education, Culture, Sports, Science and Technology (MEXT).

Supporting Information Available: Experimental details, synthetic procedures, NMR spectra, TOF-MS spectra, SEC charts, Mark–Houwink plots, modeling structure, TG curves, DSC charts, UV–vis spectra changes, AFM images, XPS spectra, cyclic voltammogram, and differential UV–vis spectra. This material is available free of charge via the Internet at <http://pubs.acs.org>.

OL900137R

(19) Men, Y.; Higuchi, M.; Yamamoto, K. *Sci. Technol. Adv. Mat.* **2006**, 7, 139.